

DYNAMIC PROPERTIES OF SAND FOR EARTHQUAKE RESPONSE ANALYSIS IN THE BAY OF CAMPECHE

Víctor Manuel Taboada Urtuzuástegui⁽¹⁾, Francisco Alonso Flores-López⁽²⁾, Diego Cruz Roque⁽³⁾, Procoro Barrera Nabor⁽³⁾, Shuang Cindy Cao⁽⁴⁾, Kwat C. Gan⁽¹⁾, Vishal Dantal⁽⁵⁾, Zianya Xarény González Ramírez⁽²⁾, Esteban Ernesto Espinosa Samudio⁽⁶⁾, Sergio Dionicio Renovato Carrión⁽⁶⁾ y Juan Manuel Hernández Durón⁽⁶⁾

ABSTRACT

The Bay of Campeche is located in a region of moderate to high seismic activity related to the active triple junction between the North American, Caribbean, and Cocos plate boundaries. Therefore, the fixed offshore platforms and subsea structures in the Bay of Campeche must be designed against earthquake loading. A database was developed of classification and index properties tests, in situ measurements of shear wave velocity (V_s) using downhole P-S suspension seismic velocity logging, in situ piezocone penetration tests, resonant column tests to characterize the shear modulus and material damping ratio at small shear strains (10^{-5} % to about 0.1 %), and strain-controlled cyclic direct simple shear tests to evaluate the decrease of shear modulus and the increase of material damping ratio at large shear strains (0.1 % to about 10 %) performed on sand from the Bay of Campeche, including sands with no carbonate content to 100 % carbonate content, retrieved from the seafloor to a penetration depth of 120 m below seafloor. The database was tailored specifically to develop empirical correlations for the Bay of Campeche sand to determine V_s when in situ measurements of V_s are not available and to develop numerical modeling to predict the variation of the normalized shear modulus (G/G_{\max}) and material damping ratio (D) as a function of shear strains (γ) when dynamic test results are unavailable for all the sand layers. The equations developed to calculate V_s and the curves of G/G_{\max} - γ and D - γ of Bay of Campeche sands are recommended for preliminary or perhaps even final seismic site response evaluations.

Keywords: Bay of Campeche; earthquake response analysis; shear wave velocity; shear modulus; material damping ratio

Artículo recibido el 09 de julio de 2021 y aprobado para su publicación el 29 de diciembre de 2022. Se aceptarán comentarios y/o discusiones hasta cinco meses después de su publicación.

⁽¹⁾ Fugro, 6100 Hillcroft Avenue, Houston, Texas 77081, USA, vtaboada@fugro.com, kgan@fugro.com

⁽²⁾ Ingenieros Geotecnistas Mexicanos (IGM), Barbero de Sevilla Mza 7 Lt 4, Agrícola Metropolitana, Tláhuac, Ciudad de México, México C.P. 13280, alonso.faf@igmmexico.com, zianya.gonzalez@igmmexico.com

⁽³⁾ Instituto Mexicano del Petróleo (IMP), Coordinación de Geotecnia Marina, Eje Central Lázaro Cárdenas Norte 152, San Bartolo Atepehuacan, Ciudad de México, México, C.P. 07730, dcruz@imp.mx, pbarrera@imp.mx

⁽⁴⁾ Changzhou University, Department of Civil Engineering, Changzhou, Jiangsu Province, 213164, China, scaocindy@163.com

⁽⁵⁾ Norwegian Geotechnical Institute (NGI), PO Box 3930 Ullevaal Stadion, N-0806 Oslo, Norway, vishal.dantal@ngi.no

⁽⁶⁾ PEMEX Exploración y Producción, Ciudad del Carmen, Campeche, México, sergio.dionicio.renovato@pemex.com, juan.manuel.hernandezd@pemex.com

PROPIEDADES DINÁMICAS DE ARENA PARA EL ANÁLISIS DE RESPUESTA SÍSMICA EN LA BAHÍA DE CAMPECHE

RESUMEN

La Bahía de Campeche se encuentra en una región de moderada a alta actividad sísmica relacionada con la triple unión activa entre los límites de las placas de América del Norte, el Caribe y la de Cocos. Por lo tanto, las plataformas fijas en alta mar y las estructuras submarinas en la Bahía de Campeche deben diseñarse contra la carga sísmica. Una base de datos de pruebas de clasificación y propiedades índice, mediciones in situ de la velocidad de la onda de corte V_s utilizando la sonda suspendida, pruebas in situ de piezocono penetrómetro (PCPT), pruebas de columna resonante para caracterizar el módulo de rigidez y la relación de amortiguación del material a bajas deformaciones angulares (10^{-5} % a aproximadamente 0.1 %) y pruebas cíclicas de corte simple directo (DSS) con deformación controlada para evaluar la disminución del módulo de rigidez y el aumento de la relación de amortiguación del material a deformaciones angulares altas (0.1 % a aproximadamente 10 %) realizados en la arena de la Bahía de Campeche incluyendo arenas sin contenido de carbonato hasta el 100% del contenido de carbonato recuperados desde el fondo marino y hasta a una profundidad de 120 m por debajo del fondo marino. La base de datos fue diseñada específicamente para desarrollar para las arenas de la Bahía de Campeche correlaciones empíricas para determinar V_s , cuando no se dispone de mediciones in situ de V_s , y modelos numéricos para predecir la variación del módulo de rigidez normalizado (G/G_{\max}) y la relación de amortiguamiento (D) de materiales en función de la deformación angular (γ) cuando no hay resultados de pruebas dinámicas disponibles para todas las capas de arena. Las ecuaciones desarrolladas para calcular V_s , y las curvas de G/G_{\max} - γ y D - γ de las arenas de la Bahía de Campeche se recomiendan para evaluaciones preliminares o tal vez incluso finales de respuesta sísmica del sitio.

Palabras Clave: Bahía de Campeche; análisis de respuesta sísmica; velocidad de onda de cortante; módulo de rigidez; relación de amortiguación del material

INTRODUCTION

The Bay of Campeche is located in the large bay comprising the southern portion of the Gulf of Mexico between the Yucatan Peninsula to the east, the Isthmus of Tehuantepec to the south, and the coast of Mexico at Veracruz to the west. It is enclosed approximately by longitude 91° W on the east, longitude 94° W on the west, latitude 20° N on the north, and the Mexican coast on the south.

The Bay of Campeche is located in a region of moderate to high seismic activity related to the active triple junction between the North American, Caribbean, and Cocos plate boundaries. Therefore, the fixed offshore platforms and subsea structures in the Bay of Campeche must be design against earthquake loading. The most important soil dynamic properties to perform earthquake response analysis include shear wave velocity (V_s), shear modulus (G_{\max}), material damping ratio (D_{\min}) at low shear strains (γ) (less than 0.0001 %), and nonlinear shear modulus (G) and material damping ratio (D) as functions of shear strain.

Unfortunately, an engineer responsible for performing earthquake response analysis in the Bay of Campeche sometimes does not have in situ measurements of shear wave velocity, and sometimes the dynamic testing performed with resonant column and strain-controlled cyclic direct simple shear (DSS) is limited and cannot be performed for all the soil layers found in the soil deposit. Therefore, the engineer has

to utilize semiempirical correlations to estimate the shear wave velocity, and the available normalized modulus reduction and damping ratio curves either are not based on marine soils or were developed for marine soils from a different geological setting with different soil characteristics from the Bay of Campeche soils.

Therefore, it was necessary to develop a database of classification and index properties tests, in situ measurements of shear wave velocity using downhole P-S suspension seismic velocity logging, in situ piezocone penetration tests (PCPTs), resonant column tests to characterize the shear modulus and material damping ratio at small shear strains (10^{-5} % to about 0.1 %), and strain-controlled cyclic DSS tests to evaluate the decrease of shear modulus and the increase of material damping ratio at large shear strains (0.1 % to about 10 %) performed on sand from the Bay of Campeche, including sands with no carbonate content to 100 % of carbonate content retrieved from the seafloor to a penetration depth of 120 m below seafloor (BSF). The database was tailored specifically to develop empirical correlations for the Bay of Campeche sands to determine V_s when in situ measurements of V_s are not available and to develop numerical modeling to predict the variation of the normalized shear modulus (G/G_{max}) and material damping ratio as a function of shear strains when no dynamic test results are available for all the sand layers.

The semiempirical correlations and the numerical modeling equations developed to determine the most important dynamic soil properties for earthquake response analysis of the marine sands of the Bay of Campeche are presented below.

SHEAR WAVE VELOCITY OF BAY OF CAMPECHE SAND

Summary of database of shear wave velocity of sand

Data were compiled from 15 sites in the Bay of Campeche, Gulf of Mexico, Mexico where in situ measurements of shear wave velocity and cone tip resistance were available. The water depths at these sites varied between 10.5 m and 80.5 m (Taboada, et al., 2015).

The soil conditions at these sites were investigated by drilling and sampling to a termination depth of 121.9 m BSF. Following completion of the drilling, sampling, and in situ testing activities, downhole P-S suspension seismic velocity logging was performed every 0.5 m from 3.0 m to 121.9 m BSF.

The range, average, and standard deviation of index and mechanical properties of the sands at the 15 sites included in the Bay of Campeche database are presented in table 1.

Table 1. Summary of index properties of sands at 15 sites.

Index property	Range	Average	Standard deviation
Carbonate content (%)	0.00 – 48.00	10.00	8.00
Water content (%)	7.00 – 53.00	28.00	7.00
Void ratio	0.44 – 1.03	0.77	0.11
Specific gravity	2.60 – 2.77	2.68	0.03
Total unit weight (kN/m ³)	17.70 – 20.60	19.40	0.60
Fines content (%)	2.00 – 50.00	14.00	10.00
Relative density (%)	13.00 – 100.00	74.00	15.00
Friction angle (degrees)	25.00 – 40.00	32.00	4.00

The relative density from the cone tip resistance (q_c) is estimated using an empirical expression proposed by Baldi, et al., (1986), which is given below:

$$D_r = \frac{1}{2.41} \ln \frac{q_c}{157(\sigma'_v)^{0.55}} \quad (1)$$

where q_c and the in situ effective vertical stress (σ'_v) are in kPa. This equation applies for normally consolidated moderately compressible, uncemented, unaged quartz sands (with 5 % or less mica by volume). Where appropriate, the cone tip resistance is corrected for the influence of fines content by using the procedures suggested by Lunne, et al. (1997).

A summary of the V_s and q_c data for the 15 sites is presented in figure 1. Representative V_s values for various D_r for given σ'_m calculated from equation (4) are plotted in figure 1a. Profiles of q_c for various D_r for given σ'_v calculated from equation (1) are plotted on figure 1b and give an indication of the state of compaction of the sand strata.

Multiple regression analyses for shear wave velocity of sand

Hardin and Richart (1963) and Richart, et al., (1970) concluded the effective mean normal stress (σ'_m) given by equation (2) and void ratio (e) are of paramount importance in determining G_{max} .

$$\sigma'_m = (\sigma'_1 + \sigma'_2 + \sigma'_3)/3 \quad (2)$$

where, σ'_1 , σ'_2 , and σ'_3 are the major, intermediate, and minor effective principal stresses, respectively. For field conditions at any given depth, $\sigma'_1 =$ effective vertical stress $= \sigma'_v$, $\sigma'_2 = \sigma'_3 = K_o \sigma'_v$, where $K_o =$ at rest earth pressure coefficient $= 1 - \sin \phi$ (where $\phi =$ drained friction angle).

Therefore, an empirical correlation similar to that proposed by Richart, et al., (1970) for rounded sand was developed. The relationship between in situ measurements of G_{max} (converted from V_s), e , and σ'_m for the Bay of Campeche sand developed through least square regression analysis to the $n = 325$ data sets is:

$$G_{max} = 8200 \frac{(2.17 - e)^2}{1 + e} (\sigma'_m)^{0.54} \quad (3)$$

where G_{max} and σ'_m are in kPa and the coefficient of correlation r^2 is 0.88. The void ratio factor $(2.17 - e)^2/(1 + e)$ proposed by Richart and coworkers based on laboratory test data also was found to be valid for the range of void ratios of the Bay of Campeche sand ($e = 0.35 - 1.0$).

An expression similar to that proposed by Seed and Idriss (1970) that relates G_{max} with effective mean normal stress and relative density was developed. The correlation based on G_{max} , σ'_m , and relative density is defined by:

$$G_{max} = 465 K_{2max} (\sigma'_m)^{0.64} \quad (4)$$

where G_{max} and σ'_m are both in kPa, K_{2max} in SI units given by equation (5), the coefficient of determination r^2 is 0.922, and the total number of data sets is $n = 340$. The corresponding values of

K_{2max} when G_{max} and σ_o are in SI units (kPa) depend on the relative density of the sand (D_r) and are given by:

$$K_{2max} = (0.6D_r + 16)/4.57 \quad (5)$$

Finally, measured values of V_s and q_c were used to calculate the ratio of normalized shear wave velocity (V_{s1}) to normalized cone tip resistance (q_{c1}). This ratio versus the normalized cone tip resistance is defined by:

$$V_s = 120(q_{c1})^{0.16} (P_a / \sigma'_v)^{-0.25} \quad (6)$$

where P_a and σ'_v are in the same units, V_s in m/s, $r^2 = 0.978$, and $n=325$. The normalized V_s is given by:

$$V_{s1} = V_s (P_a / \sigma'_v)^{0.25} \quad (7)$$

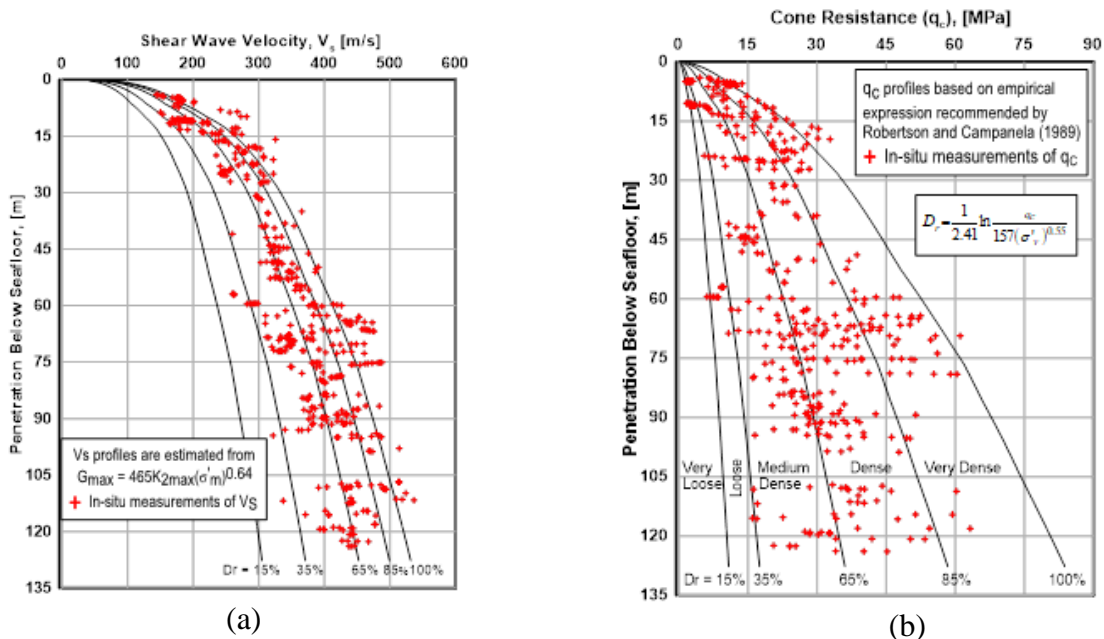


Figure 1. Summary of in situ measurements in sand of shear wave velocity (V_s) and cone resistance (q_c)

Application of the most prominent empirical correlations to determine V_s in sand

Independent, in situ measurements of V_s and q_c at a Bay of Campeche site outside of the database provided an opportunity to evaluate the accuracy of the three recommended empirical correlations to predict V_s of sand deposits presented in equations (3), (4), and (6). The correlations were directly applied to the best estimate of the correlated parameters. All the results were converted to V_s for comparison purposes.

The data shown in figure 2 indicate good agreement between the measured V_s and those inferred from the recommended equations (3), (4), and (6) for the above-mentioned site.

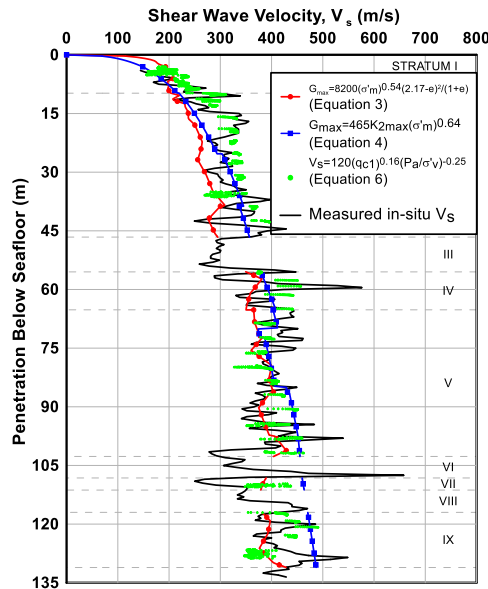


Figure 2. Blind prediction of in situ measurements of V_s in sand

Figure 2 reveals the predictions fall in a rather narrow band, 15 % lower and higher than the measured V_s , practically bounding the oscillations of the measured V_s .

The accuracy of the three empirical correlations developed to determine the shear wave velocity was investigated and found to be quite good, $\pm 15\%$ of the in-situ measurements of V_s .

G/G_{MAX}- γ AND D- γ CURVES OF BAY OF CAMPECHE SILICA SAND

Two of the most important dynamic soil properties required to conduct an equivalent-linear seismic site response analysis to evaluate the soil amplification are: i) a curve of G/G_{max} versus cyclic shear strain γ , also called modulus reduction curve, where G is the shear modulus and G_{max} is the maximum shear modulus at very low shear strains of the order of $10^{-4}\%$ and ii) a curve of equivalent hysteretic or material damping ratio D versus γ , where D is defined from the measured area (W_D) inside a complete hysteretic loop, which corresponds to the energy dissipated in one cycle, and the maximum strain energy stored during one cycle W_s , through the basic expression (see figure 3):

$$D = \frac{1}{2\pi} \frac{W_D}{G\gamma_c^2} = \frac{1}{4\pi} \frac{W_D}{W_s} \quad (8)$$

Typically, G/G_{max} decreases, and D increases as γ becomes larger, and it has been observed that a fast decrease in G/G_{max} with γ , corresponding to a strongly nonlinear soil, is associated with a strong increase of D with γ in the same soil, and vice versa.

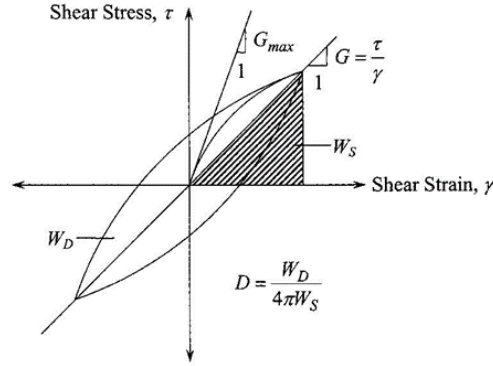


Figure 3. Hysteresis loop for one cycle of loading showing G_{max} , G , and D (Zhang, et al., 2005).

In general, G/G_{max} increase when the confining pressure (σ_m) increases. A simple way of explaining this trend is by focusing on the dependence of the shear modulus (G) on σ_m . The maximum shear modulus is defined as $G_{max} = A \sigma_m^m$, where $m = 0.4$ to 0.5 and A is a constant. For an isotropically consolidated sand, Coulomb's strength law indicates the shear strength (τ_{max}) increases linearly with σ_m ($\tau_{max} = \sigma_m \sin\phi$ for pure shear loading, where $\phi =$ angle of internal friction of the soil). Because $G = \tau/\gamma$ (figure 3), at large strains, $G = \tau_{max}/\gamma = \sigma_m \sin\phi / \gamma$; that is, G increases linearly with σ_m at large strains, whereas $G = G_{max}$ increases approximately with $\sigma_m^{0.5}$ at small strains. Therefore, G/G_{max} is proportional to $\sigma_m^{1-m} \approx \sigma_m^{0.5}$, and as σ_m increases, G/G_{max} increases. Conversely, the damping ratio (D) decreases.

It is generally difficult by any means to perform in situ tests in which large strains are imposed uniformly in the soil as it exists in the field. In realization of this, most recent efforts to pursue the strain dependency of modulus and damping of in situ soils have been directed toward the conduct of laboratory tests on undisturbed samples that are regarded as representing intact conditions in the field.

Unfortunately, it is not always possible to perform dynamic laboratory testing to obtain the shear modulus reduction curve and material damping ratio curve of all the soil strata found in the offshore soil deposit, and the geotechnical engineer is left to use curves developed mainly for onshore soils with different geological settings than those of the Bay of Campeche sand. Therefore, a characterization of the cyclic stress-strain response of the sand in shear that facilitates prediction of the shear modulus reduction curve and material damping ratio curve of sands of the Bay of Campeche is needed.

To cover this need, a database has been established and tailored for an equivalent linear characterization of the cyclic response of sand units in the Bay of Campeche. The data have been collected from offshore soil investigations performed between 2012 and 2015, which include abundant results of resonant column tests and cyclic DSS tests.

Summary of database of normalized shear modulus G/G_{max} - γ and damping $D - \gamma$ of silica sand

The existing laboratory G/G_{max} and D data of silica sand used in this study that include isotropically consolidated resonant column and strain-controlled cyclic DSS test results for 252 specimens of sand.

Histograms of the 252 specimens with respect to the water content, void ratio, relative density, fines content, carbonate content, confining pressure, coefficient of earth pressure at rest, and submerged unit weight of the specimen are presented in figure 4. As shown in figures 4a and 4b, most of the water content and void ratio of the specimens vary in the ranges of 20 % to 30 % and 0.6 to 0.8, respectively.

The relative density of the specimens (presented in figure 4c) is mostly dense in the range of 50 % to 80 %, with only 4 loose specimens with relative density below 35 % and 24 very dense specimens with relative density higher than 85 %. About 55 % of the specimens had a fines content in the range of 5 % to 10 % (figure 4d), classified as sand with silt, and about 45 % of the specimens had a fines content higher than 12 % but less than 40 %, classified as silty sand.

According to the carbonate content shown in figure 4e, about 70 % of the soil specimens are siliceous sands with carbonate content less than 10 %, and the rest of the specimens are calcareous sands with carbonate content between 10 % and 40 %. The effective confining pressures presented in figure 4f are between 100 kPa and 700 kPa, with an average of 400 kPa.

The coefficient of earth pressure at rest is mostly between 0.45 and 0.5, as observed in figure 4g, while the submerged unit weight presented in figure 4h is mostly between 20 kN/m³ and 21 kN/m³.

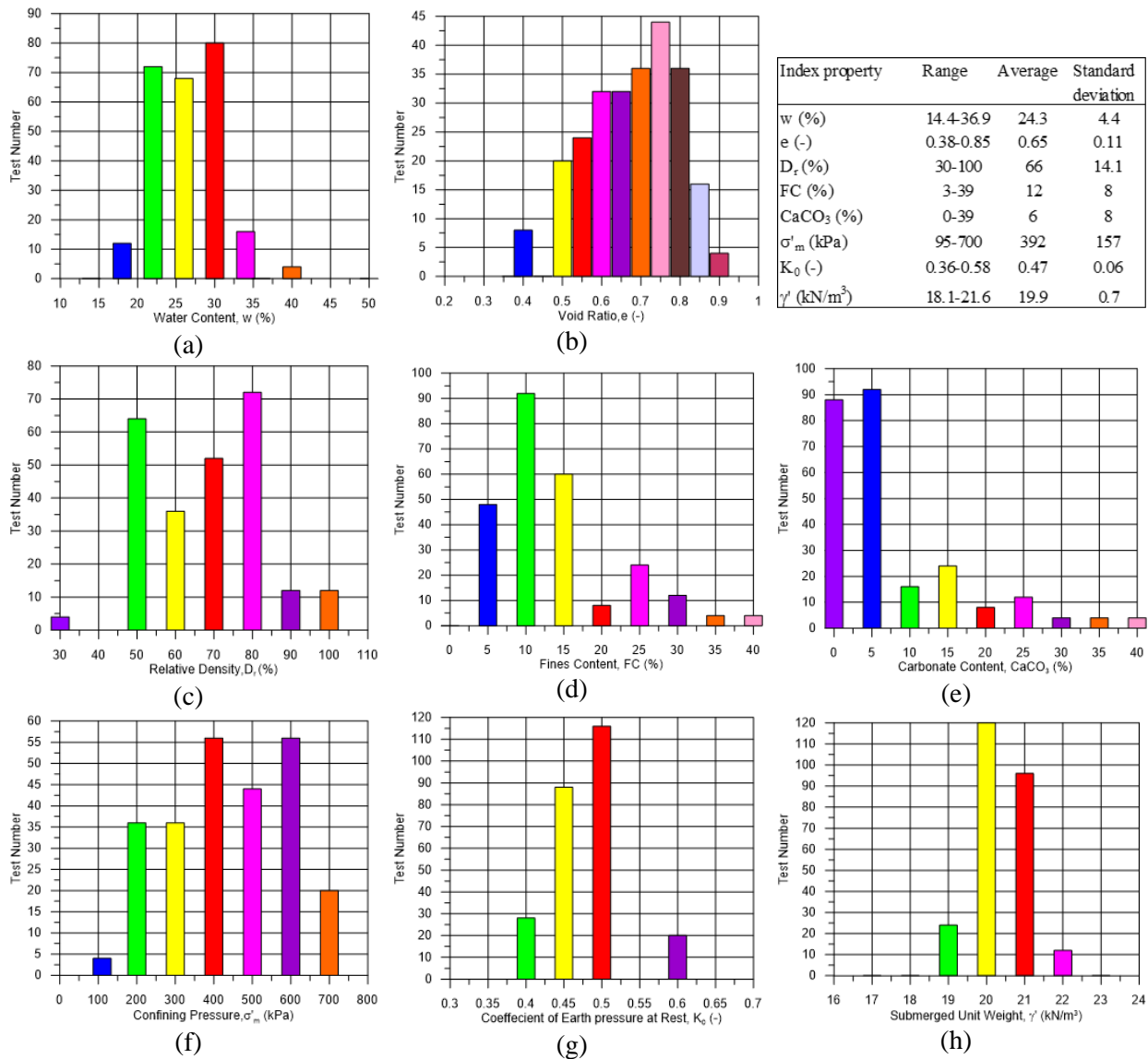


Figure 4. Histograms of the database of normalized shear modulus G/G_{max} - γ and damping D - γ of sand

Resonant column tests were performed on solid cylindrical soil specimens approximately 38 mm in diameter and 76 mm in length. Each test specimen was back-pressure saturated to about 140 kPa and then isotropically consolidated to 0.5, 1.0, and 2.0 times the in situ effective confining pressure.

Strain-controlled cyclic DSS tests were conducted on soil specimens of approximately 18 mm to 19 mm in height and trimmed to approximately 50 mm in diameter. Each granular test specimen was consolidated to an effective vertical consolidation stress equal to the estimated in situ effective vertical stress. Each test specimen was allowed to consolidate to about one log cycle of time or 24 hours, whichever was less, past the end of primary consolidation (T_{100}) before applying 20 cycles of sinusoidal cyclic horizontal loads at a frequency of 1.0 Hz (for earthquake loading conditions). The test was conducted while maintaining the specimen at a constant volume, with the pore pressures estimated by measuring the changes in the vertical stress during cycling. Each specimen was subjected to a specified nominal average cyclic shear strain of 0.25 %, 0.5 %, or 1.0 %.

In order to comprehend the non-linear elastic behavior of marine sands and to produce a best-fit functional relationship, a new database has been constructed incorporating $G/G_{\max}-\gamma$ and $D-\gamma$ curves from the Bay of Campeche sand (Taboada, et al., 2016). This curve-fitting process facilitates prediction of shear modulus degradation curves and material damping curves. The relationship between normalized shear modulus (G/G_{\max}) and shear strain (γ) for the 252 selected tests is plotted in figure 5.

Modeling of normalized shear modulus degradation curve $G/G_{\max}-\gamma$ of silica sand

The non-linear stress-strain behavior of soils at small to medium strains is mostly represented by some form of hyperbolic stress-strain relationship. Harding and Drnevich (1972) propose this relationship as:

$$\left(\frac{G}{G_{\max}}\right) = \frac{1}{1+(\gamma/\gamma_r)} \quad (9)$$

where G is the shear modulus at any strain, G_{\max} is the maximum shear modulus at $\gamma = 0.0001\%$, and γ_r is the reference shear strain, which is defined by τ_{\max}/G_{\max} . The disadvantage of this approach is the difficulty in finding τ_{\max} . The authors also indicated this true hyperbolic relationship did not generally fit their data (Harding and Drnevich, 1972).

Darendeli (2001) proposed a modified hyperbolic model based on testing on intact sand-gravel samples:

$$\left(\frac{G}{G_{\max}}\right) = \frac{1}{1+(\gamma/\gamma_r)^\alpha} \quad (10)$$

where α is called the curvature parameter and γ_r is the reference strain value at which $G/G_{\max} = 0.5$. This model uses only two parameters, and the reference strain provides an efficient normalization of shear strain. Equation (10) is adopted in this study to model the variation of G/G_{\max} with γ . For the sake of simplicity, the curvature parameter (α) is assumed independent of the effective confining pressure (σ'_m) and equal to $\alpha = 1.08$.

The best-fit functional relationship for the shear modulus degradation database is shown in figure 5 as a modified hyperbolic equation in the form proposed by Darendeli (2001) and presented in equation (10). The mean, lower-bound, and upper-bound curve-fitting parameters are:

- (a) Lower bound: $\gamma_r = 0.044\%$ and $\alpha = 1.08$
- (b) Mean: $\gamma_r = 0.080\%$ and $\alpha = 1.08$
- (c) Upper bound: $\gamma_r = 0.140\%$ and $\alpha = 1.08$

where γ_r is the reference shear strain (shear strain at $G/G_{max} = 0.5$) and α is the curvature parameter, as already defined in equation (10).

For the most common confining stresses (70 kPa to 700 kPa), the Bay of Campeche sands of this database produce a regression for γ_r as follows:

$$\gamma_r = 0.0156 \left(\frac{\sigma'_m}{P_a} \right) + 0.0277 \tag{11}$$

The resulting family of degradation curves using equation (10), varying σ'_m from 100 kPa to 700 kPa in equation (11) and considering the constant value of the curvature parameter $\alpha = 1.08$, is shown in figure 6, which leads to the interesting offsetting of the modulus degradation curves toward higher values of strain.

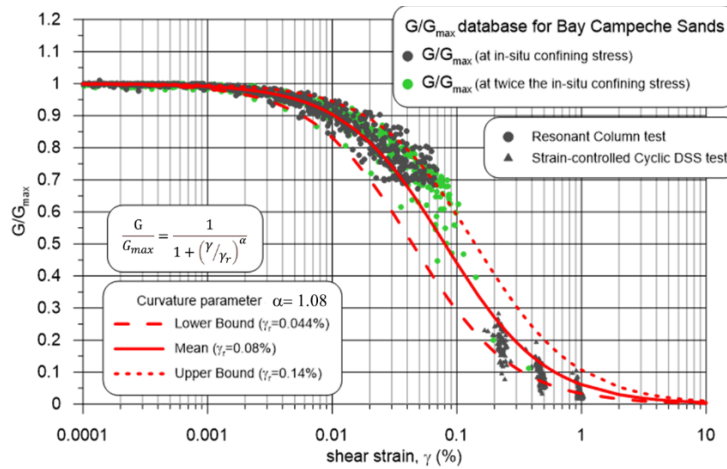


Figure 5. Fitting a hyperbola to the database of G/G_{max} and curve fitting parameters

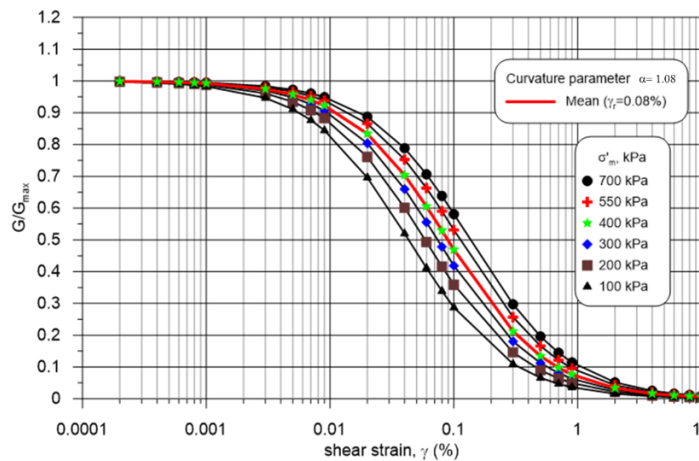


Figure 6. G/G_{max} - γ curves generated with equation (3) using $\alpha = 1.08$ and $\gamma_r = 0.08\%$

Modeling of material damping ratio curve D- γ of silica sand

The best-fit functional relationship for the material damping ratio data for the 252 selected tests is shown in figure 7 as a modified hyperbolic equation similar to that proposed by Gonzalez and Romo (2011) in the form:

$$D = (D_{max} - D_{min}) \times \left[1 - \frac{1}{1 + (\gamma/\gamma_{rD})^{\alpha_D}} \right] + D_{min} \quad (12)$$

where D_{max} and D_{min} are the maximum and minimum material damping ratios, respectively; γ_{rD} is the deformation corresponding to 50 % of increase in material damping ratio D (i.e., $D/D_{max} = 0.5$); and α_D is a curvature parameter characteristic of the curve D- γ .

For the sake of simplicity, the curvature parameter (α_D) is assumed independent of the effective confining pressure (σ'_m) and equal to 1.85.

According to the database curve fitting in figure 7, the mean, lower-bound, and upper-bound curve-fitting parameters are:

- (a) Lower bound: $\gamma_{rD} = 0.080$ % and $\alpha_D = 1.85$
- (b) Mean: $\gamma_{rD} = 0.165$ % and $\alpha_D = 1.85$
- (c) Upper bound: $\gamma_{rD} = 0.350$ % and $\alpha_D = 1.85$

The Bay of Campeche sands of this database produce regression for γ_{rD} as follows:

$$\gamma_{rD} = 0.0393(\sigma'_m/P_a) + 0.0346 \quad (13)$$

The trend of minimum material damping ratio (D_{min}) with normalized effective confining pressure produces a regression for D_{min} as follows:

$$D_{min} = 1.3492(\sigma'_m/P_a)^{-0.262} \quad (14)$$

A simple linear relation can be derived between ($D_{max} - D_{min}$) and normalized effective confining pressure using all the available data, as:

$$D_{max} - D_{min} = -0.3221 \left(\frac{\sigma'_m}{P_a} \right) + 16 \quad (15)$$

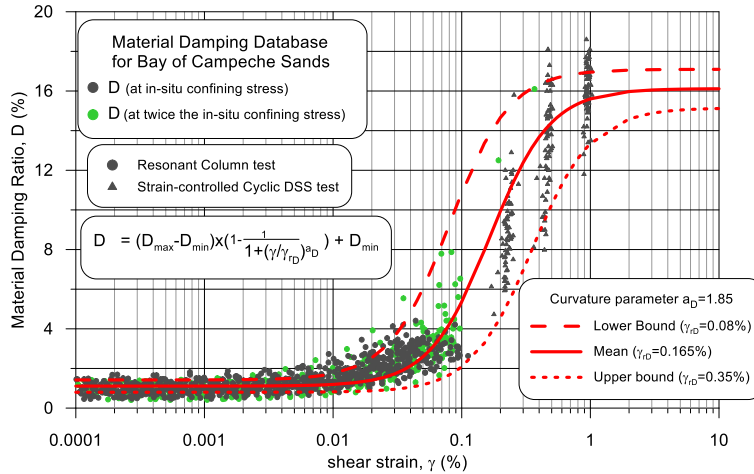


Figure 7. Fitting a hyperbola to the damping ratio databased and curve-fitting parameters

The resulting family of material damping curves using equation (12), varying σ'_m from 100 kPa to 700 kPa in equations (13), (14), and (15) and considering the constant value of the curvature parameter $a_D = 1.85$, is shown in figure 8. It leads to the offsetting of the material damping ratio curves toward higher values of strain.

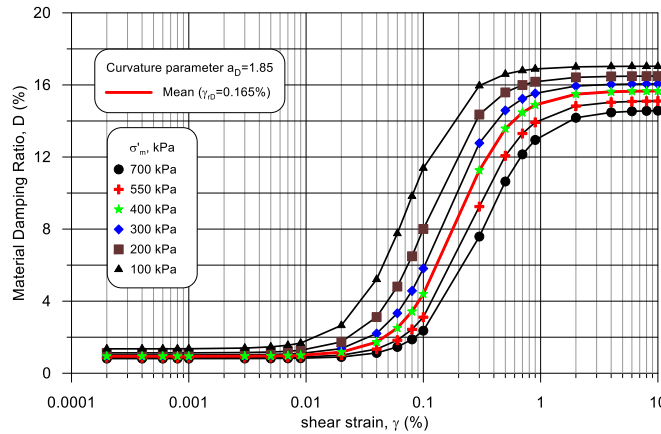


Figure 8. D - γ curves generated with equations (16) to (19) using a curvature parameter $\alpha_D = 1.85$

Validation of normalized shear modulus (G/G_{max}) and material damping ratio (D) of sand

Comparison between measured and predicted values can be validated against the database. G/G_{max} and D between predictions and measurements can best be assessed by plotting predicted against measured values for the 936 data points accumulated from all the tests. This is presented in figure 9a for G/G_{max} , where it can be seen that 85 % of the predictions lie within a factor of 1.3 and 0.7 from the measurements and values of G/G_{max} less than 0.2 are being overpredicted. The same is presented for D in figure 9b, where it can be seen that 80 % of predicted values lie within a factor of 1.3 and 0.7 from the measurements and values of D less than 4 % are being underpredicted.

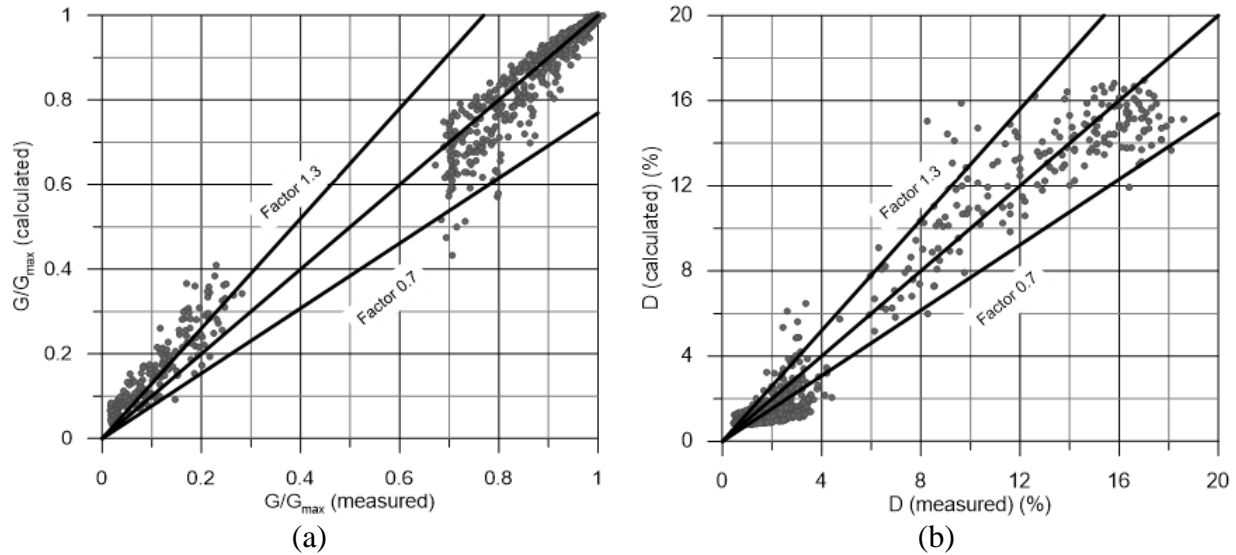


Figure 9. Comparison of 936 data points of measured and calculated values of (a) G/G_{max} and (b) D

Comparison of calculated G/G_{max} and D curves of sand with previously published curves

The calculated G/G_{max} and D curves for Bay of Campeche sands are compared with Seed and Idriss (1970), Vucetic and Dobry (1991), and Darendeli (2001) in figure 10. The recommended curves for σ'_m of 100 kPa are shown in figure 10 because the Vucetic and Dobry (1991) curves and the Seed and Idriss (1970) curves are primarily based on specimens from shallow depths (< 10 m) and are most appropriate for low confining levels corresponding to shallow depths (Roblee and Chiou, 2004). Seed and Idriss (1970) published the first database of shear modulus degradation curves and damping ratio curves for sand for the purpose of earthquake site-response analysis. The recommended G/G_{max} curve for Bay of Campeche sand presented in figure 10a for σ'_m of 100 kPa falls well between the range of G/G_{max} proposed by Seed and Idriss (1970). The recommended damping ratio curve for the Bay of Campeche sand at the same effective confining pressure presented in figure 10b closely follows the lower-bound damping curve of Seed and Idriss (1970) up to a shear strain of 0.3 %, and for shear strains higher than 0.3 % and in the range of 0.003 % to 0.07 %, the damping of the Bay of Campeche sand is lower than the lower bound of Seed and Idriss (1970).

For shear strains lower than 0.09 %, the recommended G/G_{max} curve for Bay of Campeche sand for σ'_m of 100 kPa (presented in figure 10a) is more linear than Darendeli (2001) G/G_{max} curve and Vucetic and Dobry (1991) for $PI = 0$. For shear strains higher than 0.09 %, the recommended G/G_{max} curve of Bay of Campeche sand is slightly lower than mean of Seed and Idriss (1970) and Vucetic and Dobry (1991) curves. For shear strains higher than 0.001 %, the recommended damping ratio curve for the Bay of Campeche sand for σ'_m of 100 kPa (presented in figure 10b) is lower than both Darendeli (2001) and Vucetic and Dobry (1991) damping curves and Seed and Idriss (1970) mean damping curve.

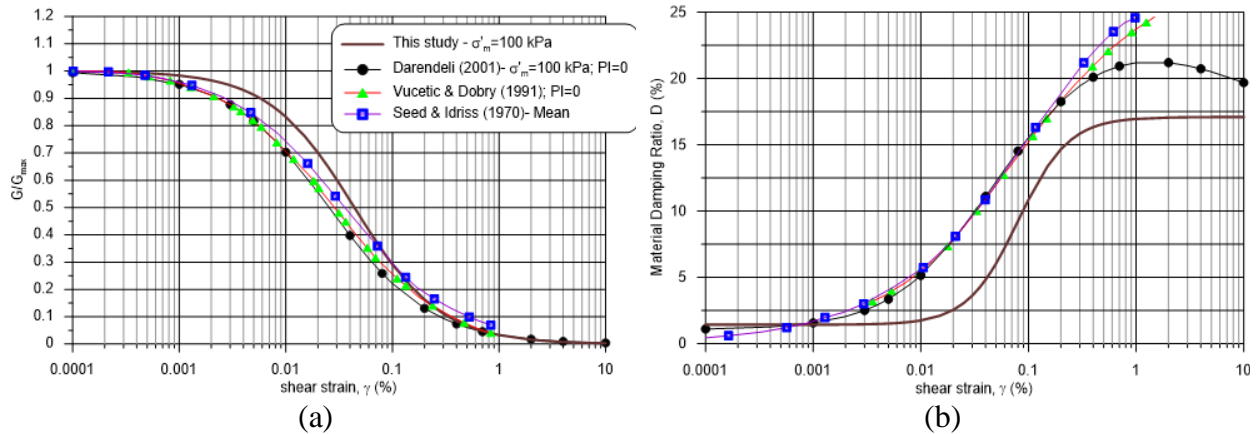


Figure 10. Comparison of recommended G/G_{max} and D curves of sand for $\sigma'_m=100$ kPa with Seed and Idriss (1970), Vucetic and Dobry (1991), and Darendeli (2001) curves

$G/G_{MAX}-\gamma$ AND $D-\gamma$ OF BAY OF CAMPECHE CALCAREOUS SAND

Summary of database of $G/G_{max}-\gamma$ and $D-\gamma$ of calcareous to carbonate sand and silt

The database of G/G_{max} and D curves used in this study was developed based on sands and silts with carbonate content higher than 10 % retrieved from the Bay of Campeche and Tabasco Coastline during geotechnical campaigns performed between 1993 and 2015 (Cruz, et al., 2015). The database contains test results of isotropically consolidated resonant column and strain-controlled cyclic DSS tests. The number of cycles of loading (N) of the cyclic DSS data is $N=15$.

Figure 11 shows histograms of 106 specimens, including graphs of carbonate content, fines content, and applied effective confining stress of Bay of Campeche calcareous to carbonate sand database. This figure shows that more than 40 % of the data presented carbonate content higher than 70 % (figure 11a), with fines content concentrated in the range of 10 % to 35 % (figure 11b), and the effective confining pressure applied to the specimens varied from 40 kPa to 1100 kPa (figure 11c).

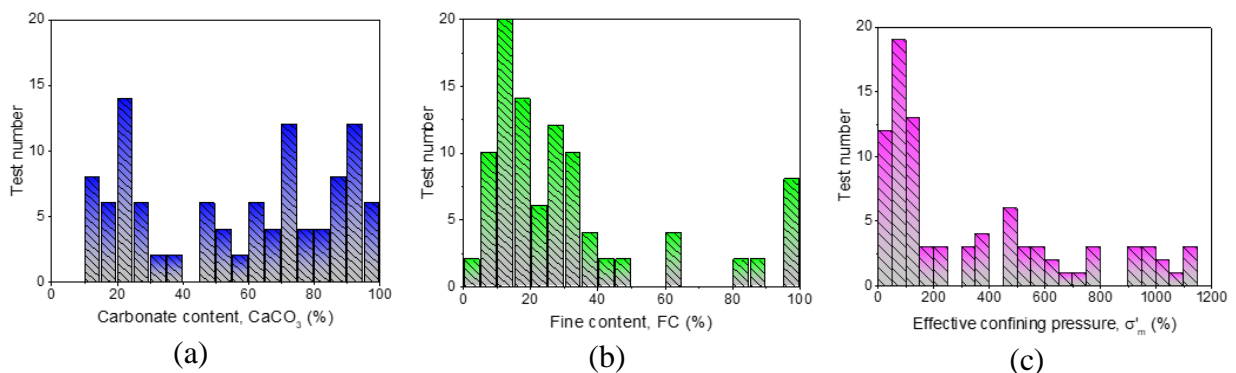


Figure 11. Histograms of (a) $CaCO_3$ and (b) FC (c) σ'_m of Bay of Campeche carbonate sand database

Figure 12 shows the database of the Bay of Campeche and Tabasco Coastline sand of 84 curves of G/G_{max} and material damping ratio (D) obtained from resonant column and cyclic DSS tests organized into two groups with carbonate content between 10 % to 50 % and 50 % to 100 % (Flores, et al., 2018). Figure

12 also presents a comparison of G/G_{max} and D curves with carbonate content higher than 10 % and curves of silica sands ($CaCO_3$ less than 10 %) of the Bay of Campeche presented by Taboada, et al. (2016). The G/G_{max} curves of sands with $CaCO_3$ higher than 10 % show a higher non-linear behavior than the silica sands. That is, G/G_{max} of carbonate sands starts to decrease at smaller cyclic shear strains than the silica sands. The damping ratio of carbonate sands is higher than silica sands, especially at cyclic shear strains smaller than 0.1 %. Figure 12 shows that as $CaCO_3$ increases, the G/G_{max} curve tends to shift downward and the damping ratio curve tends to shift upward.

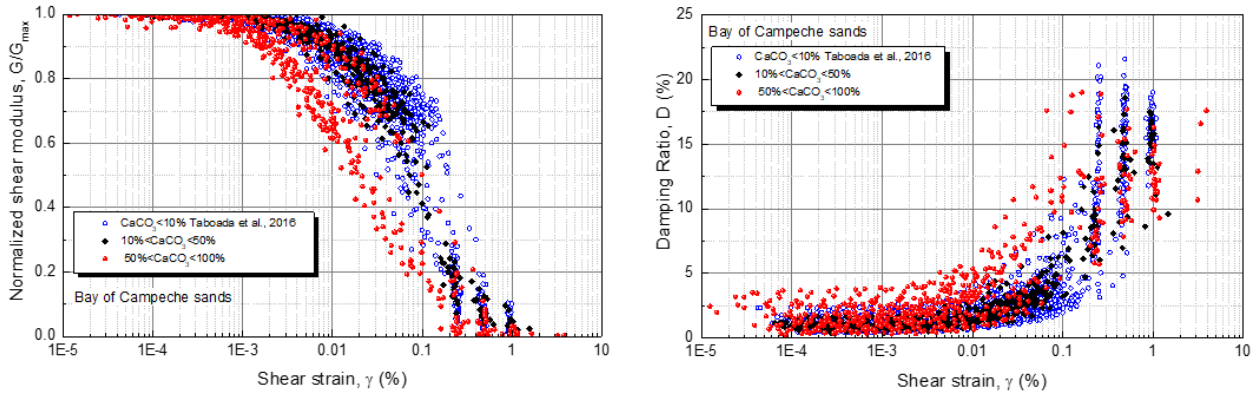


Figure 12. Comparison of normalized shear modulus G/G_{max} and damping ratio (D) of carbonate and silica sands

Modeling of G/G_{max} - γ of calcareous to carbonate sand and silt

Equation (10) was used to model the normalized shear modulus degradation curve G/G_{max} - γ , the curvature parameter (α), and reference strain γ_r that best fit the mean, upper-bound (UB), and lower-bound (LB) curves of G/G_{max} . These values were computed by regression analysis and are presented in table 2 and in figure 13 for calcareous sand, siliceous carbonate sand, carbonate sands, and silt with carbonate content between 10 % and 100 %. For simplicity, α was assumed constant and independent of effective confining pressure (σ'_m) and its values are reported in table 2.

Table 2. Parameters to best fit the curves of G/G_{max} and damping ratio of sands and marine silts

Type of soil	G/G _{max}				Damping ratio, D					
	α	γ_r (%)			α_D	γ_{rD} (%)			D_{min} (%)	D_{max} (%)
		Mean	LB	UB		Mean	LB	UB		
Calcareous sand	1.149	0.088	0.042	0.178	1.301	0.197	0.224	0.177	1.280	17.134
Siliceous carbonate sand	0.932	0.037	0.013	0.117	1.301	0.045	0.072	0.025	1.861	12.007
Carbonate sand	0.924	0.032	0.010	0.102	1.453	0.052	0.079	0.032	1.476	12.363
Silt (calcareous, siliceous carbonate and carbonate)	1.000	0.057	0.011	0.217	1.053	0.068	0.095	0.048	1.053	11.898

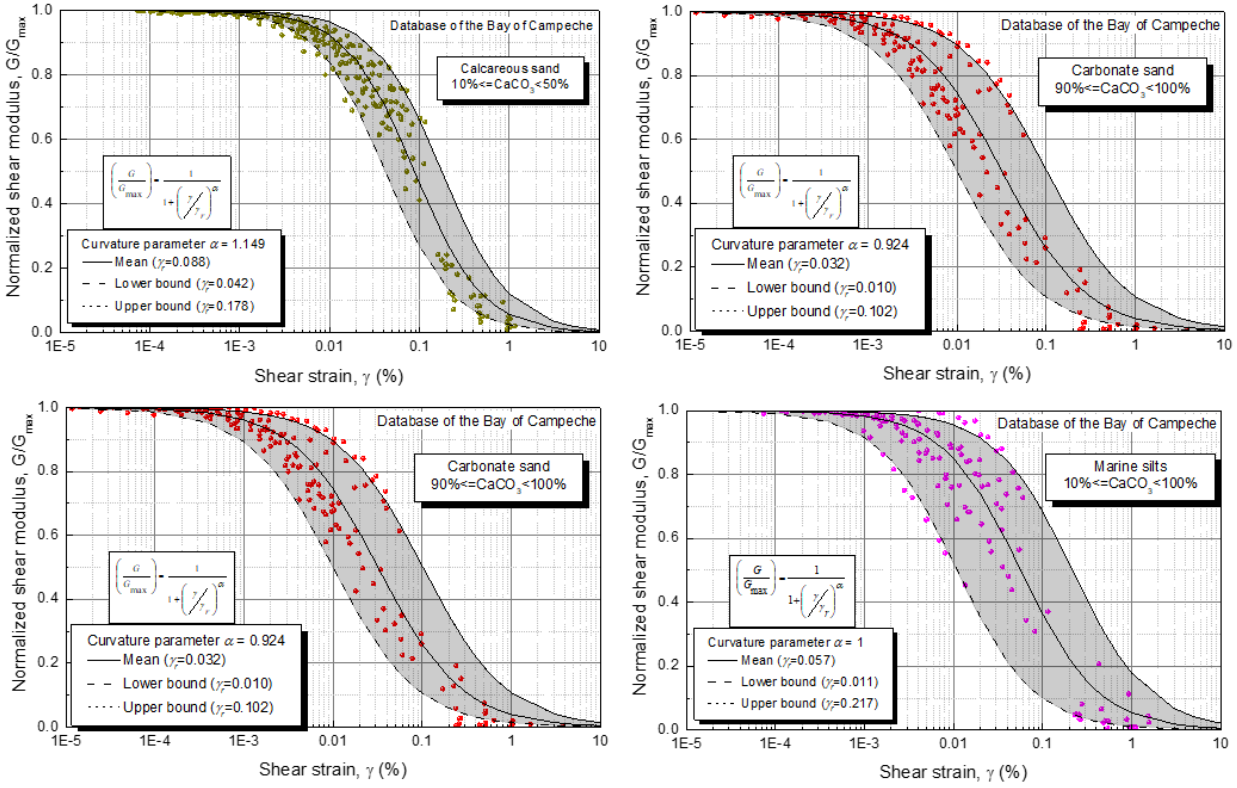


Figure 13. G/G_{max} - γ curves of (a) calcareous sand, (b) siliceous carbonate sand, (c) carbonate sand, and (d) silt

The relationship between the reference strain and the normalized effective confining pressure σ'_m with respect to the atmospheric pressure (P_a) of sands with different carbonate content was obtained. The equations for calcareous sand, siliceous carbonate sand, and carbonate sand that relate γ_r with σ'_m normalized with the atmospheric pressure (P_a) are presented below.

$$\begin{aligned} \gamma_r &= 0.0087 \left(\frac{\sigma'_m}{P_a} \right) + 0.0402 & \text{for } 10 \% \leq CaCO_3 < 50 \% \\ \gamma_r &= 0.0084 \left(\frac{\sigma'_m}{P_a} \right) + 0.0123 & \text{for } 50 \% \leq CaCO_3 < 90 \% \\ \gamma_r &= 0.0100 \left(\frac{\sigma'_m}{P_a} \right) + 0.0113 & \text{for } 90 \% \leq CaCO_3 < 100 \% \end{aligned} \quad (16)$$

Figure 14 shows the variation of the normalized shear modulus as a function of the effective confining pressure varying between 100 kPa and 1000 kPa for siliceous carbonate sand. The constant value of α (i.e. independent of effective confining pressure) presented in table 2 was used to develop the curves of normalized shear modulus as a function of effective confining pressure presented in this figure.

Figure 15 presents a comparison of the upper and lower bounds of G/G_{max} versus shear strain for silica sand, calcareous sand, siliceous carbonate sand and carbonate sand. The upper and lower bounds of G/G_{max} of silica sand are very similar to those of calcareous sands. This indicates that G/G_{max} is not significantly affected when the carbonate content is less than 50%. The upper and lower bounds of G/G_{max} of siliceous carbonate and carbonate sand are very similar, and very different than the calcareous and silica sand. This indicates that G/G_{max} is affected when the carbonate content is higher than 50%.

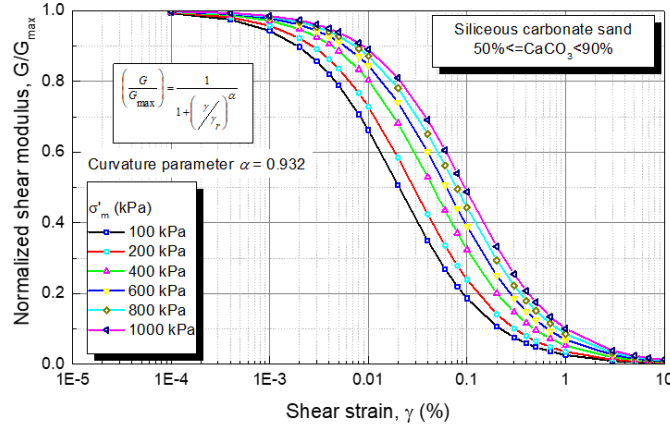


Figure 14. G/G_{\max} predicted with equations 14 and 20 as a function of σ'_m for siliceous carbonate sand

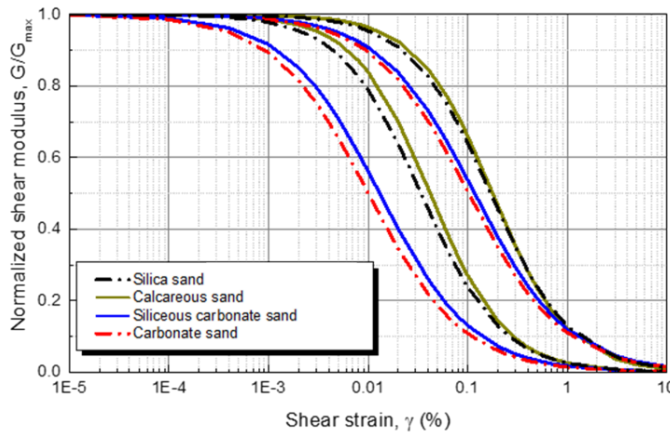


Figure 15. Comparison of upper and lower bounds of $G/G_{\max} - \gamma$ of Bay of Campeche sand

Modeling of $D-\gamma$ of calcareous to carbonate sand and silt

The database of calcareous sand, siliceous carbonate sand, carbonate sand, and silt with carbonate content between 10 % and 100 % is presented in figure 16. Equation (12) was used to define the upper bound, mean, and lower bound of the curves of damping versus shear strain presented in this figure. The values of the curvature parameter (α_D) and reference strain γ_{rD} for these three curves as well as the values of D_{min} and D_{max} that define the mean curve of damping ratio versus shear strain obtained from regression analyses are presented in table 2. For simplicity, α_D was assumed constant and independent of effective confining pressure (σ'_m), and its values are reported in table 2.

The relationships found between γ_{rD} and normalized effective confining pressure for calcareous sand, siliceous carbonate sand, and carbonate sand are presented below:

$$\begin{aligned}
 \gamma_{rD} &= 0.0444 \left(\frac{\sigma'_m}{P_a} \right) + 0.0431 && \text{for } 10 \% \leq CaCO_3 < 50 \% \\
 \gamma_{rD} &= 0.0364 \left(\frac{\sigma'_m}{P_a} \right) + 0.0189 && \text{for } 50 \% \leq CaCO_3 < 90 \% \\
 \gamma_{rD} &= 0.0476 \left(\frac{\sigma'_m}{P_a} \right) + 0.0081 && \text{for } 90 \% \leq CaCO_3 < 100 \%
 \end{aligned}
 \tag{17}$$

The relationships between minimum material damping ratio (D_{min}) with normalized confining pressure presented for carbonate sand, siliceous carbonate sand, and carbonate sand are:

$$\begin{aligned}
 D_{min} &= 1.0798(\sigma'_m/P_a)^{-0.076} && \text{for } 10\% \leq CaCO_3 < 50\% \\
 D_{min} &= 1.2090(\sigma'_m/P_a)^{-0.407} && \text{for } 50\% \leq CaCO_3 < 90\% \\
 D_{min} &= 0.9951(\sigma'_m/P_a)^{-0.372} && \text{for } 90\% \leq CaCO_3 < 100\%
 \end{aligned}
 \tag{18}$$

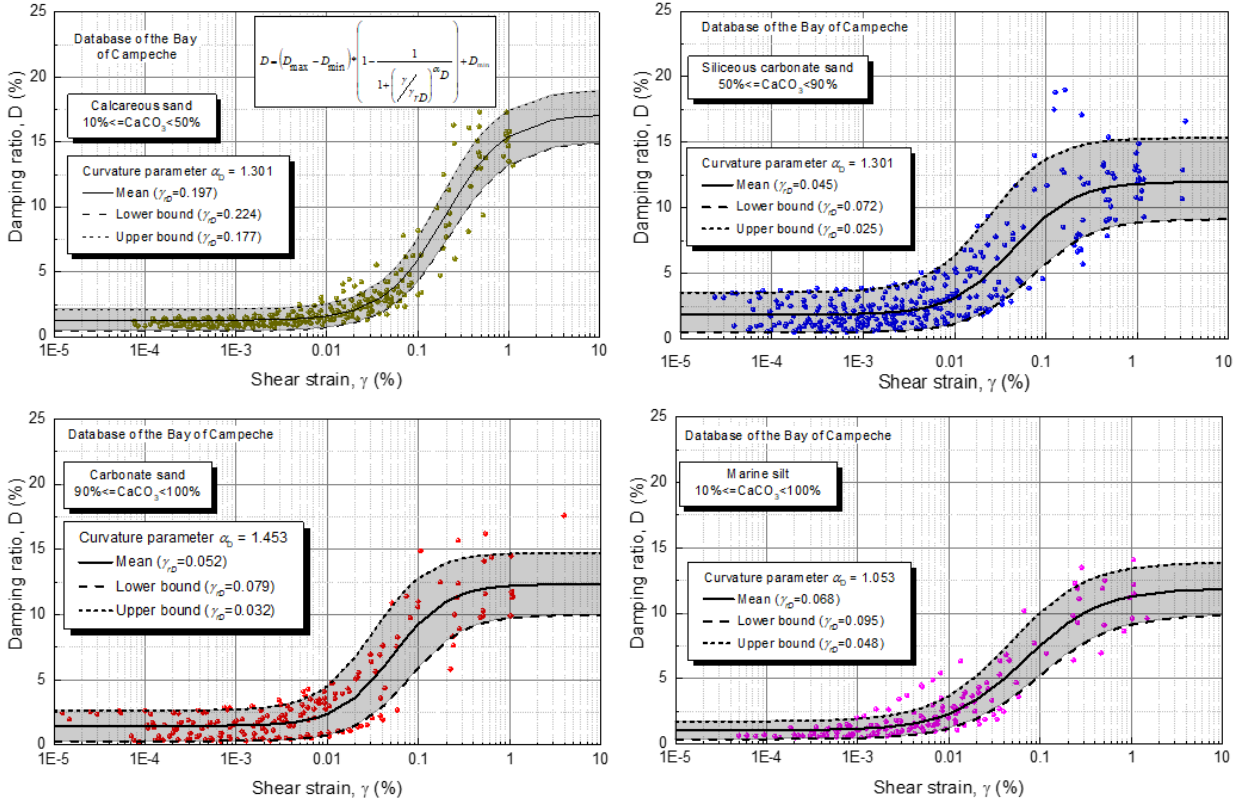


Figure 16. Curves of $D-\gamma$ of (a) calcareous sand, (b) siliceous carbonate sand, (c) carbonate sand, and (d) marine silts

The relationships between $D_{max} - D_{min}$ with normalized effective confining pressure for calcareous sand, siliceous carbonate sand, and carbonate sand are described by the following equations:

$$\begin{aligned}
 D_{max} - D_{min} &= -0.6298 \left(\frac{\sigma'_m}{P_a} \right) + 18.342 && \text{for } 10\% \leq CaCO_3 < 50\% \\
 D_{max} - D_{min} &= -0.4192 \left(\frac{\sigma'_m}{P_a} \right) + 15.169 && \text{for } 50\% \leq CaCO_3 < 90\% \\
 D_{max} - D_{min} &= -0.015 \left(\frac{\sigma'_m}{P_a} \right) + 11.955 && \text{for } 90\% \leq CaCO_3 < 100\%
 \end{aligned}
 \tag{19}$$

Figure 17 shows the variation of material damping ratio versus cyclic shear strain with effective confining pressure for siliceous carbonate sand. The curvature parameter (α_D) was considered independent of the effective confining pressure, and its constant value is presented in table 2.

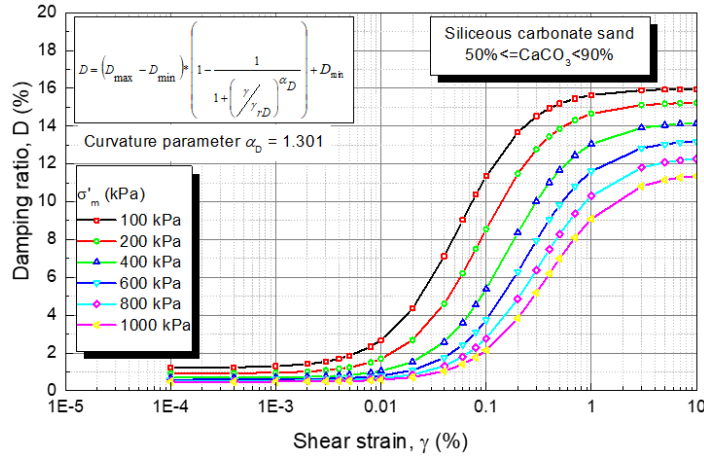


Figure 17. Prediction of D - γ with equations (16), (21), (22), and (23) for various σ'_m for siliceous carbonate sand

Figure 18 shows a comparison of the upper and lower bounds of damping ratio versus shear strain for silica sand, calcareous sand, siliceous carbonate sand, and carbonate sand of the Bay of Campeche and Tabasco Coastline. The damping curves of silica sand and carbonate sand are very similar, although the bandwidth is smaller in calcareous sand than in silica sand. The curves of siliceous carbonate sand and carbonate sand are very similar and show a different shape and width than the curves of silica sand and calcareous sand. This indicates there is a small effect on the curve of damping ratio when the carbonate content is smaller than 50 % and an important effect when the carbonate content is greater than 50 %. The damping ratio of siliceous carbonate and carbonate sands is higher than the calcareous and silica sands at shear strains smaller than about 0.1 % and shows an asymptotic value at shear strains larger than 0.4 %.

Validation G/G_{max} and material damping ratio (D) of calcareous to carbonate sand

Figure 19a shows the comparison of 902 measurements of G/G_{max} using resonant column and strain-controlled cyclic DSS and calculated values of G/G_{max} using equations (10) and (16) for the three ranges of carbonate content of sand considered in this study (calcareous sand, siliceous carbonate sand, and carbonate sand). This figure shows a 1:1 line illustrating that the calculated value is equal to the measured value and this line multiplied by a factor of 0.7 (30 % underprediction) and 1.3 (30 % overprediction). There is excellent agreement between the measured and calculated values of G/G_{max} for the case of resonant column data ($G/G_{max} = 1.0$ to $G/G_{max} = 0.2$). The measured values of G/G_{max} with strain-controlled cyclic DSS tests are over predicted in most of the cases, especially for measured values of $G/G_{max} < 0.1$.

ISSN-e-2395-8251

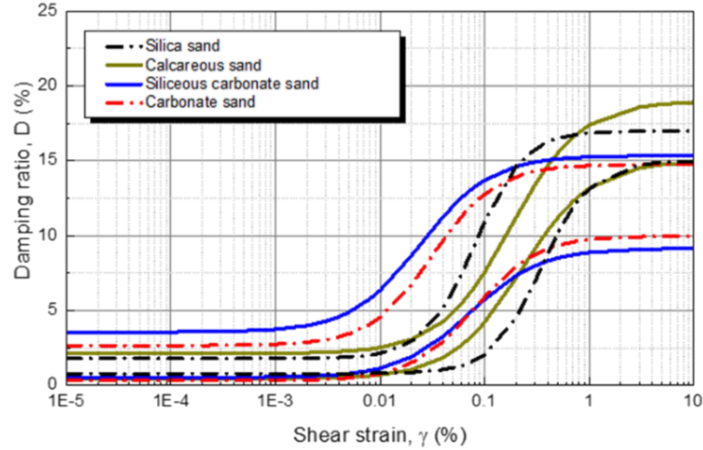


Figure 18. Comparison of upper and lower bound of damping ratio of sands with different carbonate contents

Figure 19b presents the measured versus predicted damping ratio for calcareous sand, siliceous carbonate sand, and carbonate sand for a total of 902 measured points. A good prediction is observed when the measured damping ratio is greater than 4 %, mostly falling within a band of $\pm 30\%$ of the measured values. However, the equation underpredicts the damping ratio measured at lower shear strains with the resonant column test for measured values of $D < 4$.

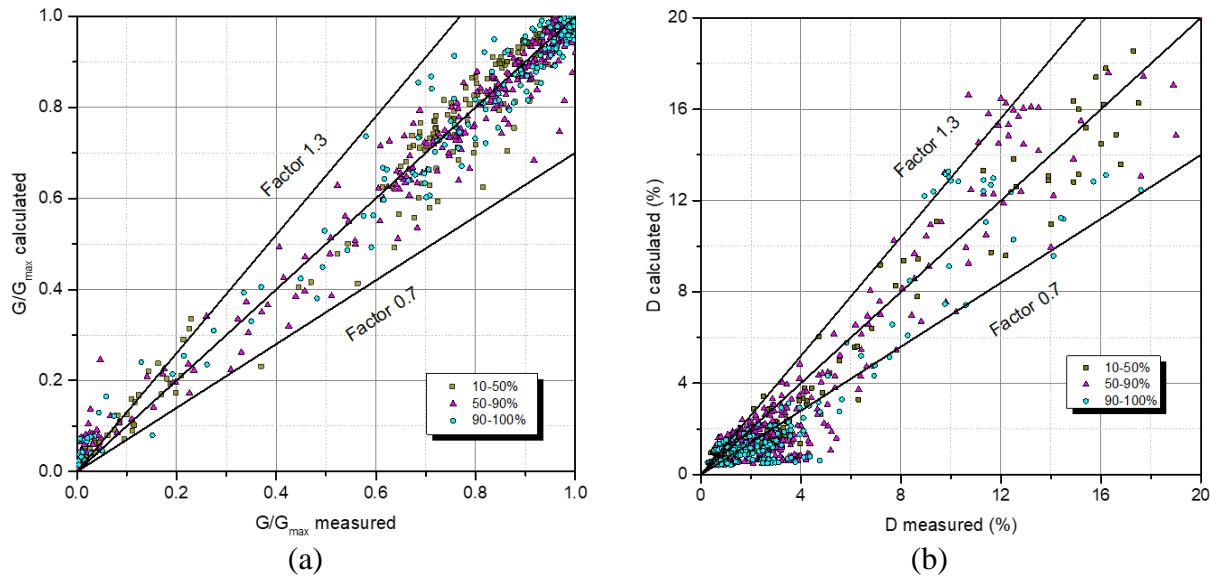


Figure 19. Measured and predicted G/G_{max} and D for carbonate sand, siliceous carbonate sand, and carbonate sand

CONCLUSIONS AND RECOMMENDATIONS

A database of in situ V_s measurements with a P-S suspension seismic velocity logger and standard geotechnical engineering material properties for the Bay of Campeche sand has been established. The database allowed the development of several empirical correlations between in situ V_s , basic soil properties of sand, and cone net resistance. These equations should be used with caution in predicting the in-situ shear

wave velocity in the top 3.5 m because there were no V_S measurements in these surficial soils due to the noise transmitted from the vessel to the time records used for V_S determination, which made shear wave arrivals difficult to pick. It is recommended the predictions of V_S made with the relationships in the top 3.5 m should be limited to the lowest value of 35 m/s.

The following 3-step procedure is recommended to determine the three V_S profiles of clay and sand needed to perform earthquake response analysis in the Bay of Campeche when in situ measurements of V_S at the site are not available:

- First, develop the best estimate in situ V_S profile in clay by calculating the average of the three V_S values estimated using equations (10), (12), and (14) presented in Taboada, et al., (2013).
- Second, develop the best estimate in situ V_S profile in sand by calculating the average of the three V_S values estimated using equations (3), (4), and (6).
- Third, to incorporate the potential for variation in the site conditions and the uncertainties in the best estimate in situ shear wave velocity three different shear wave velocity profiles must be analyzed for each acceleration time history: the best estimate V_S , a lower V_S case, and a higher V_S case. The lower and higher V_S cases are estimated by applying scaling factors of $(2/3)^{1/2} = 0.816$ and $(3/2)^{1/2} = 1.225$ to the best estimate in situ shear wave profiles obtained in the previous two steps. These scaling factors are recommended in ASCE 4-98 (1998).

A database of resonant column and strain-controlled cyclic DSS tests was developed for the following soil types: sand, calcareous sand, siliceous carbonate sand, and carbonate sand. The database allowed the development of predicting equations based on two independent modified hyperbolic relationships to determine the normalized shear modulus G/G_{\max} - γ and material damping ratio D - γ curves when no dynamic test results are available for a given soil layer within the strata.

The predictive equation of G/G_{\max} in the form of equation (10) features two curve-fitting parameters: reference strain γ_r at $G/G_{\max} = 0.5$ and a curvature parameter α . For simplicity, the curvature parameter α was given a constant value for sands. A linear relation for sand, between the reference strain γ_r and the normalized effective confining stress with respect to the atmospheric pressure, σ'_m/P_a , were established for the most common range of effective confining stresses ($\sigma'_m = 50 \text{ kPa} - 1,200 \text{ kPa}$).

The predictive equation of material damping ratio in the form of equation (12) features four curve-fitting parameters: reference strain γ_{rD} at $D/D_{\max} = 0.5$; a curvature parameter α_D characteristic of the curve D - γ ; and maximum and minimum material damping ratios, D_{\max} and D_{\min} , respectively. For simplicity, the curvature parameter α_D was given a constant value for sand. A linear relation for sand, between the reference strain γ_{rD} and the normalized effective confining stress with respect to the atmospheric pressure, σ'_m/P_a , were established. An exponential relation for sand, was established between σ'_m/P_a , and D_{\min} . A linear relation between $(D_{\max} - D_{\min})$ and σ'_m/P_a for sand was established.

It is shown that as CaCO_3 increases, the G/G_{\max} curve tends to shift downward and the damping ratio curve tends to shift upward and the influence in the shape of the G/G_{\max} is evident when the carbonate content is higher than 50 %.

The validation of the calculated values of G/G_{\max} and D shows the best predictions are found at low shear strains for G/G_{\max} and at large shear strains for D falling within $\pm 25 \%$ of the measured values. Due to the limitations in the model at large strains ($\gamma > 1 \%$) for G/G_{\max} and at low strains ($\gamma < 0.05 \%$) for D , the calculated values fall within $\pm 50 \%$ of the measured values.

Comparisons between the predictive equations developed in this study and the earlier previously published curves show the predictive equations of this study of G/G_{\max} exhibits the most linear response and the largest threshold shear strain, and beyond the threshold strain the curve degrades at the highest rate. The predictive equations of material damping ratio provide the lowest material damping ratio for cyclic shear strains larger than 0.001% for sand.

The equations developed to calculate V_s , and the curves of $G/G_{\max}-\gamma$ and $D-\gamma$ of Bay of Campeche sands are recommended for preliminary or perhaps even final seismic site response evaluations. It has been shown that they can be used in practice to perform earthquake response analysis in the Bay of Campeche and determine the design acceleration spectrum at the depth of maximum soil-pile interaction (Taboada, et al., 2022).

However, considering the scatter of the data points around V_s and the curves, the equations should be used with caution, and parametric and sensitivity studies are strongly recommended to assess the importance of this scatter. In large critical projects, in situ measurements of V_s and direct experimental determinations of G/G_{\max} and D for the sands of interest are suggested to be more appropriate.

ACKNOWLEDGEMENTS

This research was made possible thanks to the work performed offshore by roughnecks, drillers, engineers, laboratory technicians, and marine crew to collect high-quality soil samples in the Bay of Campeche; the onshore dynamic laboratory testing performed by the laboratory technicians at Fugro's Houston laboratory; and the quality assurance and quality control of the test results performed by onshore engineers in Houston. Their dedication and skills are greatly appreciated.

REFERENCES

- American Society of Civil Engineers, ASCE 4-98 (1998). *Seismic analysis of safety-related nuclear structures and commentary on standard for seismic analysis of safety related nuclear structures*. <https://doi.org/10.1061/9780784404331>
- Baldi, G, R Bellotti, V Ghionna, M Jamiolkowsky & E Pasqualini (1986). "Interpretation of CPTs and CPTUs, 2nd Part: Drained Penetration in Sands". *4th Int. Geotechnical Seminar Field Instrumentation and In Situ Measurements* (pp 143–156). Nanyang Technical Institute.
- Cruz, D, M Lopez, F A Flores, P Barrera, E Rojas, R Torres, M Cervantes, J M Hernández & S Renovato (2015). "System information of geophysical and geotechnical data of marine soils of the Gulf of Mexico". *Proceedings of the XV Panamerican Conference of Soil Mechanics and Geotechnical Engineering, Buenos Aires, Argentina, November*.
- Darendeli, B M (2001). "Development of a new family of normalized modulus reduction and material damping curves". *Doctoral dissertation*, University of Texas.
- Flores Lopez, F A, V M Taboada, Z X Gonzalez, D Cruz, P Barrera & V S Dantal (2018). "Normalized modulus reduction and damping ratio curves for Bay of Campeche carbonate sand". *Offshore Technology Conference*. <http://dx.doi.org/10.4043/29010-MS>
- Gonzalez, C M & M P Romo (2011). "Estimación de propiedades dinámicas de arcillas". *Revista de Ingenieria Sismica*, 84, 1–23. <http://dx.doi.org/10.18867/RIS.84.19>

- Hardin, B O & V P Drnevich (1972). “Shear modulus and damping in soils: Measurement and Parameter Effects (Terzaghi Lecture)”. *Journal of the Soil Mechanics Foundation Division, ASCE*, 98(7), 667–692. <https://doi.org/10.1061/JSFEAQ.0001756>
- Hardin, B O & F E Richart (1963). “Elastic wave velocities in granular soils”. *Journal of the Soil Mechanics Foundation Division, ASCE*, 89(SM1), 33–65. <https://doi.org/10.1061/JSFEAQ.0000493>
- Lunne, T, P K Robertson & J J M Powell (1997). *Cone penetration testing in geotechnical practices*. Blakie Academic & Professional, London, p. 312.
- Richart, F E, J R Hall & R D Woods (1970). *Vibrations of soils and foundations*. Prentice-Hall.
- Roblee, C & B Chiou (2004). “A proposed geindex model for design selection of non-linear properties for site response analysis”. *Proceedings of the NSF/PEER International Workshop on Uncertainties in Nonlinear Soil Properties and their Impact on Modeling Dynamic Soil Response*. University of California.
- Seed, H B & I M Idriss (1970). *Soil moduli and damping factor for dynamic response analyses*. Report No. EERC 70-10, EERC. University of California.
- Taboada, V M, D Cruz, P Barrera, E Espinosa, D Carrasco & K C Gan (2013). “Predictive equations of shear wave velocity for Bay of Campeche clay”. *Proceedings of the 45th Offshore Technology Conference*. <http://dx.doi.org/10.4043/24068-MS>
- Taboada, V M, D Cruz, P Barrera, S D Renovato, J M Hernández & K C Gan (2015). “Predictive equations of shear wave velocity for Bay of Campeche Sand”. *Proceedings of the third International Symposium on Frontiers in Offshore Geotechnics III* (pp. 1115–1120). Taylor & Francis Group.
- Taboada, V M, V Dantal, D Cruz, F A Flores & P Barrera (2016). “Normalized modulus reduction and damping curves for Bay of Campeche sand”. *Offshore Technology Conference*. <http://dx.doi.org/10.4043/26878-MS>.
- Taboada, V M, S H Cao, D Cruz, P Barrera & F A Flores (2022). “Using predicted Dynamic properties to perform seismic site response analyses on a Bay of Campeche calcareous soil deposit”. *Offshore Technology Conference*. <http://dx.doi.org/31809-MS>.
- Vucetic, M & R Dobry (1991). “Effect of soil plasticity on cyclic response”. *Journal of Geotechnical Engineering*, 117(1), 89–107. [https://doi.org/10.1061/\(ASCE\)0733-9410\(1991\)117:1\(89\)](https://doi.org/10.1061/(ASCE)0733-9410(1991)117:1(89))
- Zhang, J, R D Andrus & C Hsein Juang (2005). “Normalized shear modulus and material damping ratio relationships”. *Journal of Geotechnical and Geoenvironmental Engineering, ASCE*, 131(4). [https://doi.org/10.1061/\(ASCE\)1090-0241\(2005\)131:4\(453\)](https://doi.org/10.1061/(ASCE)1090-0241(2005)131:4(453))